

Micromechanics of non-active clays in saturated state and DEM modelling

Arianna Gea Pagano^{1,*}, Alessandro Tarantino¹, Matteo Pedrotti¹, Vanessa Magnanimo², Kit Windows-Yule² and Thomas Weinhart²

¹ University of Strathclyde, Department of Civil and Environmental Engineering, Glasgow, UK

² University of Twente, Faculty of Engineering Technology, Multi-Scale Mechanics (MSM), Enschede, Netherlands

Abstract. The paper presents a conceptual micromechanical model for 1-D compression behaviour of non-active clays in saturated state. An experimental investigation was carried out on kaolin clay samples saturated with fluids of different pH and dielectric permittivity. The effect of pore fluid characteristics on one-dimensional compressibility behaviour of kaolin was investigated. A three dimensional Discrete Element Method (DEM) was implemented in order to simulate the response of saturated kaolin observed during the experiments. A complex contact model was introduced, considering both the mechanical and physico-chemical microscopic interactions between clay particles. A simple analysis with spherical particles only was performed as a preliminary step in the DEM study in the elastic regime.

1 Introduction

Microstructure of discrete materials such as soils affects the macroscopic behaviour of the material itself. The Discrete Element Method (DEM), first proposed by Cundall and Strack ([1]) is a numerical technique that can be successfully used in order to simulate those aspects of soil behaviour that cannot be anticipated at the scale of the sample, although derivable from the particle scale. Two of the many issues that need to be addressed in the application of the DEM for clayey geomaterials are ([2]): a) physico-chemical microscopic interactions between particles have to be taken into account as well as conventional mechanical interactions and b) the plate-like (3D) or rod-like (2D) shape of clay particles plays a key role in the interpretation of soil macroscopic behaviour and cannot be ignored during the analysis.

The paper presents an experimental investigation carried out on saturated kaolin clay samples in order to assess the effect of the pore fluid characteristics affecting kaolin's microstructure on the one-dimensional compressibility of the soil. A micro-mechanical conceptual model was estimated from the experimental observations and used as a basis for a three dimensional DEM analysis, considering both mechanical and physico-chemical microscopic interactions. A simple preliminary analysis with spherical particles only was performed in order to reproduce qualitatively some of the microscopic mechanisms concerning the elastic behaviour of the sample. Further simulations can be performed using rod-like and plate-like particles, already implemented in the model, in order to explore the effect of particles shape on the compressibility behaviour in the plastic regime.

2 Experimental investigation

2.1. Background

Electrochemical interactions existing between kaolin clay particles (mainly Coulomb and van der Waals interactions) are known to control the macroscopic behaviour of non-active clays. Such interactions affect particles arrangement, and are affected by both pH and dielectric permittivity.

Pore fluid pH has been proven to affect the distribution of charges on kaolin particles edges. While particle surfaces are assumed to be permanently negatively charged due to isomorphic substitution of cations with negative charges ([3], [4]), particles edges can be either positively or negatively charged due to protonation/deprotonation of broken edges induced by changes in pH ([3], [5], [6]). For low pH values (acid solutions), the face-to-face interaction is repulsive while the edge-to-face interaction is attractive. This charge distribution leads to open structures. For high pH values (alkaline solutions), both face-to-face and edge-to-face interactions are repulsive. This charge distribution leads to close structures.

On the other hand, dielectric permittivity is assumed to affect the extent of Coulomb repulsive forces existing between particle faces. By considering two facing particles as two circular plates, the repulsive force F [N] can be calculated as ([7]):

$$F = \frac{\pi a^2}{8\epsilon} \rho^2 \left(\frac{d}{\sqrt{a^2 + d^2}} - 1 \right) \quad (1)$$

* Corresponding author: arianna.pagano@strath.ac.uk

where a is the radius of the plates [m], d is the plates distance [m], ρ is the electrical charge distribution on the two plates [C/m^2] and ε is the dielectric permittivity of the media between the two plates [F/m], defined as the vacuum permittivity times the relative permittivity.

2.2. Experimental setup

Four cylindrical Speswhite kaolin samples of 100 mm diameter and different heights were tested in a modified triaxial cell apparatus. A cylindrical splitting mould was used to give the required shape to the samples and avoid lateral deformations during the tests. Each sample was saturated with a different pore fluid prior to the test, in order to assess the effect of pore fluid pH and dielectric permittivity on the one dimensional compressibility behaviour. The properties of each sample are shown in Tables 1 and 2.

A loading frame was used to load/unload the samples in oedometric loading condition. A constant strain rate, slow enough to guarantee drained conditions during the test, was applied continuously at the bottom of the cell. A load cell was used to measure the applied force.

Table 1. Samples tested to assess the effect of permittivity.

Test n°	Height [mm]	Pore fluid	Pore fluid content [%]	Dielectric permittivity
1	74.9	Air (dry sample)	100	1
2	83.3	Ethanol	100	25
3	84.3	Deionised water	100	80

Table 2. Samples tested to assess the effect of pH.

Test n°	Height [mm]	Pore fluid	Pore fluid content [%]	pH
3	84.3	Deionised water	100	4
4	91.9	Water + dispersant	55	9

2.3. Experimental results

Figure 1 shows the one dimensional compressibility curves obtained for the four reconstituted samples. By comparing the results of tests 1-2-3 and tests 3-4 the effect of dielectric permittivity and pH of the pore fluid respectively can be investigated.

2.3.1 Effect of dielectric permittivity

The compressibility curves for tests 1-2-3 show a different behaviour during loading and unloading-reloading cycles. Samples having lower values of dielectric permittivity show higher void ratio values e , defined as the ratio between the volume of voids and the volume of solids, for the same vertical effective stress,

σ' , as a consequence of the higher repulsive force developed between particles. However, upon loading (irreversible volume change), the lower the permittivity, the more compressible is the sample. Upon unloading-reloading (reversible volume change), this trend is reversed: samples having low dielectric permittivity swell less than samples with high dielectric permittivity and, hence, are less compressible upon reloading.

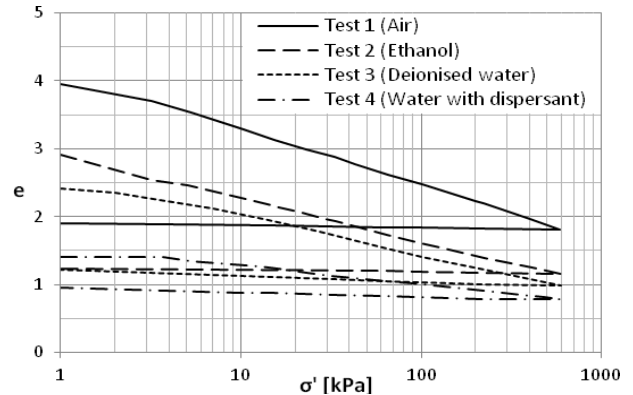


Fig. 1. One dimensional compressibility curves

2.3.2 Effect of pH

The compressibility curves for tests 3-4 show the effect of pH during loading and unloading-reloading cycles. Upon loading, the sample saturated with demineralised water at pH4 (test 3) exhibits higher values of void ratio and a much more compressible behaviour than the sample saturated with water and dispersant at pH9 (test 4). Upon unloading, the swelling of the two samples appears to be very similar, although there is still a difference in void ratio.

2.4. Micro-mechanical conceptual model as a basis for the DEM analysis

For both pH-induced configurations (edge-to-face and face-to-face), the lower the pore fluid dielectric permittivity the “stiffer” is the microscopic contact between particles, i.e. the higher is the repulsive force developed for the same particles distance. This affects the initial macroscopic configuration of the soil: the lower the dielectric permittivity, the more open is the structure and the higher is the void ratio. However, samples with open microscopic structures exhibit a more compressible behaviour at the macroscopic scale in the plastic regime (first loading). Loading can cause the destruction of some of the edge-to-face contacts between particles: the more open is the structure, the higher is the loss in terms of void ratio every time an edge-to-face contact is permanently lost upon first loading, leading to a faster drop of void ratio with applied load. Vice versa, in the elastic regime (unloading-reloading), the swelling-compressibility behaviour is affected by the “stiffness” of the particles contact only: highly repulsive contacts (low dielectric permittivity) will reduce swelling upon unloading and compressibility upon reloading.

3 DEM analysis

3.1. DEM implemented model

The micro-mechanical conceptual model previously introduced was implemented in a three dimensional DEM analysis.

A modified contact model was introduced in order to take into account both mechanical and physico-chemical microscopic interactions (Figure 2). The first interaction is conventionally defined in DEM analyses as the relationship between the overlap of particles in contact, δ_{ij}^n , and the repulsive contact force in the normal direction, f_{ij}^n , developing when overlapping occurs ($\delta_{ij}^n > 0$). The second interaction has to be defined as the relationship between the particles distance ($\delta_{ij}^n < 0$) and the attractive/repulsive force developing before the overlap occurs. These “long range” forces will be used to mimic the effect of Coulomb interaction, either repulsive or attractive, and van der Waals interaction, generally assumed to be attractive for clay particles. The total force acting on the particles is obtained by adding together these three contributions, calculated as follows:

$$f_{ij}^n = \begin{cases} 0, & \delta_{ij}^n < 0 \\ k_n \delta_{ij}^n, & \delta_{ij}^n > 0 \end{cases} \quad (2)$$

$$f_{ij,coul}^n = \begin{cases} 0, & \delta_{ij}^n < \delta_{ij}^{n,1} \\ k_{coul}(\delta_{ij}^n - \delta_{ij}^{n,1}), & \delta_{ij}^{n,1} < \delta_{ij}^n < \delta_{ij}^{n,2} \\ k_{coul}(\delta_{ij}^{n,2} - \delta_{ij}^n), & \delta_{ij}^n > \delta_{ij}^{n,2} \end{cases} \quad (3)$$

$$f_{ij,vdw}^n = \begin{cases} 0, & \delta_{ij}^n < \delta_{ij}^{n,2} \\ k_{vdw}(\delta_{ij}^n - \delta_{ij}^{n,2}), & \delta_{ij}^{n,2} < \delta_{ij}^n < 0 \\ k_{vdw}(0 - \delta_{ij}^{n,2}), & \delta_{ij}^n > 0 \end{cases} \quad (4)$$

where k_n is the stiffness of the particles themselves (always positive), k_{coul} is the stiffness of Coulomb interaction $f_{ij,coul}^n$ (either positive or negative), k_{vdw} is the stiffness of van der Waals interaction $f_{ij,vdw}^n$ (assumed to be negative), and $\delta_{ij}^{n,1}$ and $\delta_{ij}^{n,2}$ are the lower limits of Coulomb and van der Waals interaction range respectively.

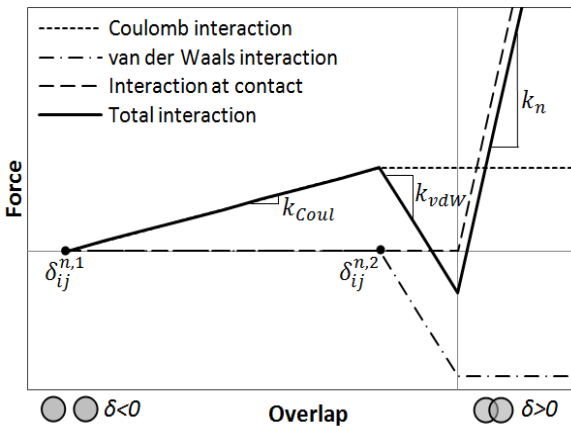


Fig. 2. Qualitative example of the implemented contact model

As regards the particles shape, three possible solutions have been implemented: spherical, rod-like and plate-like particles (Figure 3). For rods and platelets, each particle interacts with the surrounding particles with the previously mentioned contact law, plus an additional attractive interaction that glues together particles belonging to the same rod or platelet.

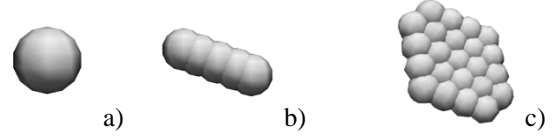


Fig. 3. Particle shape: a) spherical, b) rod-like and c) plate-like

3.2. DEM simulations: setup

Three preliminary simulations were performed using 3D assemblies of spherical particles only. Each simulation consists in an initial isotropic compression from gas state, followed by a sample relaxation after a solid state condition is reached and a 1D compression in the z direction. In order to guarantee the homogeneity of the samples, the simulations were performed using periodic boundary conditions and a constant strain rate during each stage.

The simulations were performed using assemblies of 400 particles. Particle diameters were randomly chosen between 0.5 and 1.2×0.5 m. For sake of simplicity, van der Waals interactions were ignored during the simulations and only repulsive (positive) Coulomb interactions were considered for negative δ_{ij}^n values. The parameters defining the contact law for each simulation are shown in Table 3.

Table 3. Contact model parameters.

Simulation n°	k_n [N/m]	k_{Coul} [N/m]	k_{vdw} [N/m]	$\delta_{ij}^{n,1}$ [m]	$\delta_{ij}^{n,2}$ [m]
1	1×10^6	0	0	0	0
3	1×10^6	100	0	1	0
4	1×10^6	500	0	1	0

3.3. DEM simulations: results and discussion

3.3.1 Preparation and relaxation

The three samples were isotropically compressed up to the same target value of elastic energy (energetically defined gas/solid transition criterion) and then relaxed. As expected, the higher the repulsive stiffness k_{coul} , the sooner the target value was reached (Figure 4). After preparation, a relaxation stage was performed in order to reach a stable, quasi-static condition. The quasi-static condition was identified and guaranteed energetically by relaxing the sample until a target value of elastic energy to kinetic energy ratio was reached.

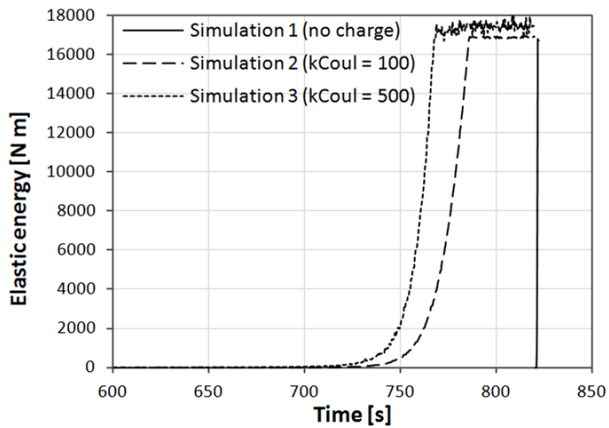


Fig. 4. Elastic energy versus time during preparation/relaxation

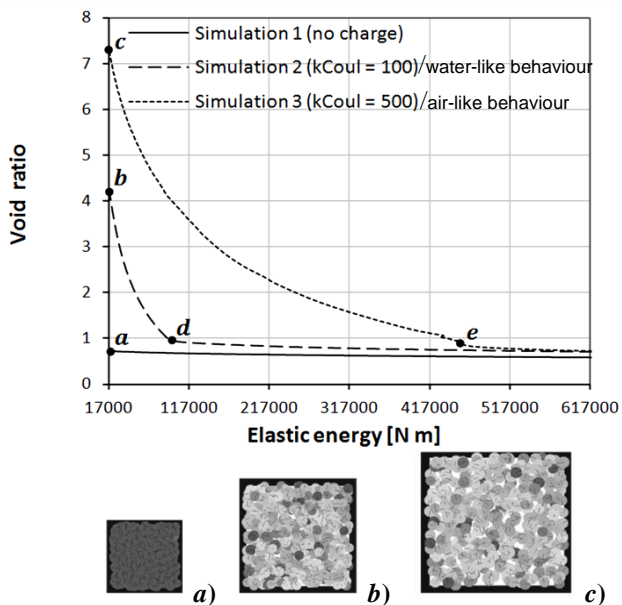


Fig. 5. Void ratio versus elastic energy during 1D compression

3.3.2 One dimensional compression

Figure 5 shows the evolution of void ratio with elastic energy during vertical 1D compression for the three simulations. The extent of the repulsion affects both the sample configuration and the energetic response during compression. The initial void ratio, corresponding to the last step of the relaxation stage, increases significantly with k_{Coul} : highly repulsive particles reach the gas/solid transition stage arranging themselves in a more open structure than weakly repulsive or non repulsive particles (Figure 5 a, b, c). Upon loading, the sample with no Coulomb interactions (simulation 1) shows the least compressible behaviour, since its compressibility depends on the value of k_n only. For simulations 2 and 3, the higher the k_{Coul} the less compressible is the sample. After reaching a threshold void ratio value, the slope of the compressibility curve becomes almost parallel to the one obtained for simulation 1 (points d, e in Figure 5). This change in trend occurs when charged particles, initially interacting only in the $\delta_{ij}^n < 0$ range, come into contact: at this point, the compressibility of

the whole system will be mainly depending on k_n , whose order of magnitude is much higher than the one of k_{Coul} .

The void ratio versus elastic energy curve can be qualitatively compared to the compressibility curves obtained experimentally. Elastic energy gives a measure of the confining pressure acting on the particles in the main direction of loading and, hence, can give us an idea of the effective vertical stress existing in the sample. Since spherical particles are not adequate to predict any of the edge-to-face and face-to-face configuration mechanisms occurring in kaolin samples during first loading, conclusions can be drawn about the elastic behaviour only. The results obtained in the simulations confirm the trend observed during the experiments when assessing the effect of dielectric permittivity: the higher the repulsion, i.e. the lower the dielectric permittivity, the lower the compressibility in the elastic regime.

4 Conclusions

An experimental investigation was carried out in order to assess the effect of pH and dielectric permittivity on the one dimensional compressibility of kaolin clay samples. Two different microscopic mechanisms have been assumed to take place during the tests: a configuration-induced effect, occurring during first loading, and a charge-induced effect, occurring during unloading-reloading cycles.

A simple preliminary set of DEM simulations with spherical particles only and a suitable modified contact model was already able to simulate the microscopic mechanism occurring during unloading-reloading cycles. Further simulations need to be performed using rod-like and plate-like particles, in order to explore the effect of particles shape on the compressibility behaviour in the plastic regime.

References

1. P. A. Cundall, O. D. Strack, *Geotechnique*, **29**, 47-65 (1979)
2. M. Yao, A. Anandarajah, *J. Of Eng. Mech.*, **129**, 585-596 (2003)
3. J. Mitchell, K. Soga, *Fundamentals of Soil Behavior* (John Wiley and Sons Inc. Hoboken, NJ, 2005)
4. Y. H. Wang, W. K. Siu, *Can. Geot. J.*, **43**, 587-600 (2006)
5. B. Rand, I. E. Melton, *J. of Coll. and Int. Sc.*, **60**, 308-320 (1977)
6. H. Van Olphen, *Clay Colloid Chemistry: For Clay Technologists, Geologists and Soil Scientists* (John Wiley, 1977)
7. M. Pedrotti, PhD thesis, University of Strathclyde (2015)